In vitro synergistic activity of cisplatin and EGFR-targeted nanomedicine of anti-Bcl-xL siRNA in a non-small lung cancer cell line model

Phuoc Vinh Nguyen, Katel Hervé-Aubert, Laurie Lajoie, Yoann Misericordia, Igor Chourpa, Stéphanie David, Emilie Allard-Vannier

International Journal of Pharmaceutics: X 4 (2022) 100139

Contents lists available at ScienceDirect

International Journal of Pharmaceutics: X

journal homepage: www.sciencedirect.com/journal/international-journal-of-pharmaceutics-x

In vitro synergistic activity of cisplatin and EGFR-targeted nanomedicine of anti-Bcl-xL siRNA in a non-small lung cancer cell line model☆

Phuoc Vinh Nguyen [a,b], Katel Hervé-Aubert [a], Laurie Lajoie [c], Yoann Misericordia [a], Igor Chourpa [a], Stéphanie David [a], Emilie Allard-Vannier [a,*]

[a] EA6295 Nanomédicaments et Nanosondes, Université de Tours, Tours, France
[b] School of Medicine, Vietnam National University Ho Chi Minh city, Ho Chi Minh city, Viet Nam
[c] ISP UMR1282, INRAE, équipe BioMAP, Université de Tours, Tours, France

ARTICLE INFO

Keywords:
NSCLC
EGFR-targeted nanomedicine
BcL-xL
Cisplatin
Gene delivery
scFv

ABSTRACT

Apoptosis is an important process that directly affects the response of cancer cells to anticancer drugs. Among different factors involved in this process, the BcL-xL protein plays a critical role in inhibiting apoptosis induced by chemotherapy agents. Henceforth, its downregulation may have a synergistic activity that lowers the necessary dose of anticancer agents. In this study, anti-Bcl-xL siRNA were formulated within an EGFR-targeted nanomedicine with scFv ligands (NM-scFv) and its activity was tested in the non-small cell lung cancer (NSCLC) cell line H460. The obtained NMs-scFv anti-Bcl-xL were suitable for intravenous injection with sizes around 100 nm, a high monodispersity level and good siRNA complexation capacity. The nanocomplex's functionalization with anti-EGFR scFv ligands was shown to allow an active gene delivery into H460 cells and led to approximately 63% of gene silencing at both mRNA and protein levels. The NM-scFv anti-Bcl-xL improved the apoptotic activity of cisplatin and reduced the cisplatin IC_{50} value in H460 cells by a factor of around three from 0.68 ± 0.12 μM to 2.21 ± 0.18 μM ($p < 0.01$), respectively, in comparison to that of NM-scFv formulated with control siRNA ($p > 0.05$).

1. Introduction

Lung cancer is the leading cause of cancer-related deaths in the world, with approximately 1.8 death cases in 2020 (18% of all death cases caused by cancer) (Bade and Dela Cruz, 2020; Ferlay et al., 2021). It is a heterogenous cancer that can be divided into two principal forms including non-small cell lung cancer (NSCLC) and small-cell lung cancer (SCLC) (Osmani et al., 2018). NSCLC represents approximately 85% of all lung cancer patients, and around 40% of patients suffering from this subtype are at an advanced stage when they are diagnosed (Herbst et al., 2018; Osmani et al., 2018).

Due to the comorbility caused by NSCLC, several treatment strategies have been developed and proven their effectiveness, including radiotherapy, chemotherapy, targeted therapy, immunotherapy or the combination of them. Despites these efforts, the 5-year survival of NSCLC remains relatively low (approximately 20–30%) because of diagnosis at advanced stages (Min and Lee, 2021). Furthermore, the conventional chemotherapy remains the mainstay treatment option for NSCLC despite of the remarkable progress in immunotherapy with anti-PD1 and anti-PDL1 agents. However, the drug resistance phenomenon is silently emerging and poses a direct threat to the treatment effectiveness (Kim, 2016; Sosa Iglesias et al., 2018). Different mechanisms of chemotherapy resistance have been studied and demonstrated in NSCLC, such as i) an enhancement in DNA repair capacity by upregulating ERCC1 or DNA polymerase, in drug efflux by activating several drug export transporters (ATP7A/B, ABCC1/MRP1, ABCC3/MRP3, P-gp), in drug detoxification by increasing the intracellular concentration of glutathione, in pro-survival signal pathways (EGFR, STAT3, PI3k/Akt, MAPK, NF-kB), and in EMT- a related factor to the metastasis or ii) a decrease in drug uptake by down-regulating Na^+/K^+-ATPase pumb or CTR1 protein, in cell cycle arrest by an overexpression in anti-apoptotic proteins (Bcl-xL, Bcl-2) (Kim, 2016; Min and Lee, 2021; Mirzaei et al., 2021a; Sosa Iglesias

Abbreviations: scFv, single chain variable fragment; NSCLC, non-small cell lung cancer; EGFR, epidermal growth factor receptor; BcL-xL, B-cell lymphoma-extra large.

☆ This article was originally submitted to IJP on 02-March-22 but the paper was transferred to IJP:X on 11-Nov-2022.

* Corresponding author.
E-mail address: emilie.allard@univ-tours.fr (E. Allard-Vannier).

https://doi.org/10.1016/j.ijpx.2022.100139

Available online 13 November 2022

et al., 2018).

Among different chemotherapy agents used for NSCLC patients, platinum compounds with cisplatin (CIS) as the gold standard is the main treatment regimen. It can be administered in combination with third-generation anticancer drugs such as gemcitabine, vinorelbine or taxanes (Alexander et al., 2020; Šutić et al., 2021). However, its application is more and more limited by severe side effects and a drug-resistance phenomenon, such as the overexpression of anti-apoptotic proteins that leads to an impair in apoptosis in cancer cells (Duma et al., 2019; Huang et al., 2007). Indeed, CIS causes DNA damages and induces cellular apoptosis, involving the upregulation of apoptotic proteins such as Bax or Bak and the downregulation of anti-apoptotic proteins (BcL-2 and Bcl-xL) (Huang et al., 2007; Lei et al., 2007; Zhang et al., 2018). It has been proven that the overexpression of Bcl-xL and Bcl-2 can delay the apoptosis process caused by several cytotoxic drugs including CIS (Huang et al., 2007; Lei et al., 2007). In fact, CIS causes the cell death and cell cycle arrest through the formation of DNA lesion that can be delayed or even deactivated by the overexpression of Bcl-xL. Therefore, the downregulation of such anti-apoptotic proteins may have a therapeutic activity on cancer cells' sensitivity to anticancer drugs (Kim et al., 2004).

Gene therapy involving small interfering RNAs (siRNAs) has emerged as one of the most promising solutions for the specific down-regulation of these cancer-related proteins (Fire et al., 1998; Singh et al., 2018; Subhan and Torchilin, 2019). siRNAs' mechanism of action is based on their interfering activity with cancer-associated target genes that leads to the protein downregulation and contributes actively to an enhancement in the therapy efficiency. siRNAs can bring about substantial benefits to cancer therapy thanks to their potency, specificity and ability to target any cancer-related genes (Lochmatter and Mullis, 2011; Vinh Nguyen et al., 2020). In case of cisplatin, several studies have proven the potency of siRNAs in reversing cisplatin resistance by down-regulating several important tumor-promoting factors such as EZH2, H1F-1a, EGFR, STAT3, Nrf2, ID1, Nek2, Akt1 (Mirzaei et al., 2021a). Despite their potential, naked siRNA applications are unfeasible in clinical settings due to their intrinsic nature and because of the presence of intra- and extracellular barriers (Ben Djemaa et al., 2018; Vinh Nguyen et al., 2020). For extracellular barriers, naked siRNAs are prone to be degraded by nucleases in the bloodstream or eliminated by renal clearance (Mirzaei et al., 2021b). In terms of intracellular barriers, even if they can escape from enzymatic degradation, there is a high chance that their highly negative charges hinder their penetration through the negative cell membrane into their final active site (cytoplasm). For all previous reasons, siRNAs need to be delivered by an appropriate system and nanomedicines are one of the most promising siRNA carriers (Ben Djemaa et al., 2019).

The current study is performed to apply a novel nanomedicine that has been previously developped and optimized by our team in the active delivery of anti-Bcl-xL siRNAs into NSCLC cells. Our nanomedicine is functionalized with anti-EGFR scFv ligands to target EGFR-overexpressing H460 cells (Vinh Nguyen et al., 2020). The EGFR is a receptor in the family of tyrosine kinases that is strictly related to cancer development, metastasis and resistance (Dhomen et al., 2012; Mansour et al., 2018; Tan et al., 2016; Van den Eynde et al., 2011). The EGFR-overexpression is a common phenomenon and can be observed up to 80% in NSCLC cases (Liang et al., 2010; Salimath et al., 2015; Vinh Nguyen et al., 2021). Taking into account the EGFR-overexpression and the important role of Bcl-xL in NSCLC treatment, anti-Bcl-xL siRNAs were complexed with our targeted nanomedicine (NM-scFv). Afterwards, the Bcl-xL downregulation at both the transcriptional and translational levels induced by our NM-scFv was assessed and compared to a non-targeted nanomedicine (NM). The therapeutic activity of the finalized NM-scFv was then evaluated by an apoptosis assay in combination or not with cisplatin. Finally, the synergistic activity of our targeted nanomedicine combined with cisplatin was studied using a cell viability assay.

2. Materials and methods

2.1. Preparation of targeted nanomedicine with anti-EGFR scFv ligands for anti-Bcl-xL siRNA delivery

2.1.1. Synthesis of the targeted nanovector (NV-scFv)

The NV-scFv's synthesis was based on our previously published protocol including three steps: (i) the coupling of a near-infrared fluorescent dye onto the silanized SPION's surface, (ii) the covering of the silanized SPIONs with a polyethylene glycol (PEG) layer and (iii) the functionalization of the PEGylated SPIONs with 100% humanized anti-EGFR scFv ligands (Vinh Nguyen et al., 2020).

2.1.2. Formulation of the targeted nanomedicine (NM-scFv)

Anti-Bcl-xL siRNA (sequence 5′-GACUGUGGCCGGCGUGGUU/AAC-CACGCCGGCCACAGUC-3′, Sigma-Aldrich, St. Quentin Fallavier, France) and scramble or control siRNA (Ambion®, New-York, U.S.A) were complexed with NVs-scFv and two cationic polymers namely chitosan (MW = 110–150 kDa, degree of acetylation ≤40 mol%) and poly-*L*-arginine (PLR, MW = 15–70 kDa, Sigma-Aldrich Chimie GmbH, St. Quentin Fallavier, France), to obtain the corresponding NM-scFv anti-Bcl-xL and NM-scFv control, respectively, according to the previously published protocol (Vinh Nguyen et al., 2020). Briefly, siRNAs were precomplexed with PLR while chitosan was mixed with NVs-scFv. The complexed siRNA/PLR was then added into the mixture of NV-scFv/chitosan and homogenized using micropipette mixing and vortexing. The final siRNA concentration was fixed at 50 nM for internalization assay, 100 nM for qRT-PCR and Western blot assays, and 2000 nM for physico-chemical characterization. The mass ratio (MS) was used to determine the NV-scFv/siRNA ratio. The cationic polymers' content was defined as the charge ratio or the molar ratio of the positive charges of polymers and the negative charges of siRNA. All these ratios were optimized in our previous publication and fixed at 10 to obtain the optimal siRNA transfection efficiency (Vinh Nguyen et al., 2020).

2.2. Physico-chemical characterization

2.2.1. Size and zeta potential analysis

The hydrodynamic diameter (D_H), the polydispersity index (PDi), and the zeta potential (ζ) were determined using a Nanosizer apparatus (Zetasizer®, Malvern Instrument, UK). The measurement was performed in $NaNO_3$ 0.01 M to fix the ionic strength. The D_H was based on intensity measurements and were achieved at 25 °C. All measurment were performed in triplicate.

2.2.2. siRNA complexation capacity

To verify the siRNA complexation capacity of our NMs-scFv, the electrophoresis technique on agarose gel was employed. An agarose gel at 1% (m/v) was prepared containing 0.01% (*v*/v) of ethidium bromide (EtBr) to visualize free siRNA. NMs and NMs-scFv were formulated twice at 2000 nM in siRNA. The first sample of each formulation was diluted with water and the second was diluted with heparin 10 g/L at a dilution factor of 2:1 (v/v). A loading buffer was added and a final content corresponding to 16 pmol of siRNA per well was deposited. The migration of samples on the gel was conducted in a Tris-acetate-EDTA (TAE) 1× buffer for 15 min at 150 V. The visualization of free siRNA was made with UV-imaging using the EvolutionCapt software on a Fusion-Solo.65.WL imager (Vilber Lourmat, Marne-La-Vallée, France).

2.3. Cell culture experiments

2.3.1. Cell culture

Luciferase stably expressing human non-small cell lung cancer (H460-Luc) was a gift from CIPA TAAM CNRS UPS44, Orléans, France. H460-Luc cells were cultured at 37 °C in an atmosphere containing 5% of CO_2. The culture medium was made of RPMI-1640 medium

supplemented with 10% of FBS, 2 mM of L-glutamine, 1% of penicillin/streptomycin. Cell harvesting was carried out with trypsin/EDTA (0.05%) at 80% of confluence.

2.3.2. Internalization assay

The cellular internalization level of NMs and NMs-scFv into H460-Luc cells was determined and compared by tracking the near-infrared fluorescence from grafted dyes on NVs (Dylight™680 dye) using flow cytometry. H460-Luc cells were seeded in a 12-well plate at 1.5×10^5 cells/well. After 24 h, NMs and NMs-scFv prepared with anti-Bcl-xL siRNAs in reduced-serum Opti-MEM were added to the cells at a final concentration of 50 nM in siRNA (or 6.58 mg of iron/L) for 4 h. After 4 h, a cell culture medium of 20% of serum was added at a dilution factor of 1:1 (*v*/v) for 20 h. Non-treated cells were used as negative controls. After 24 h, the cells were washed, harvested, and analyzed by flow cytometry (Gallios flow cytometer, Beckman Coulter, U.S.A). All experiments were triplicated and treated using Flowing Software 2.5.1 (Turku Bioscience Centre, Turku, Finland).

2.3.3. Cell transfection

H460-Luc cells were seeded at 3×10^6 cells/well in 6-well plates for 24 h. On the transfection day, anti-Bcl-xL siRNAs were complexed within Lipofectamine™ RNAiMAX, NMs, and NMs-scFv and diluted with serum-reduced medium Opti-MEM at a dilution factor of 1:10 (v/v) to obtain the siRNA finalized concentration of 100 nM. Afterwards, the culture medium was removed, and the cells were washed twice with the HBSS buffer. 1 mL/well of each formulation with complexed siRNAs was added and the transfection was performed for 4 h. The negative control was made with Opti-MEM without adding siRNA. After 4 h, 1 mL of the culture medium enriched in serum (20%) was added and maintained at 37 °C for another 20 h for qRT-PCR analysis or 44 h for Western Blot assay.

2.3.4. RNA extraction and qRT-PCR analysis

At 24 h after cell transfection, total-RNAs were isolated from cultured cells using the NucleoSpin RNA kit (Macherey-Nagel, Hoerdt, Germany) according to the manufacturer's protocol, and subsequently reverse transcribed into complementary DNAs (cDNAs) by the RevertAid First Strand cDNA Synthesis Kit (Thermo Scientific™, Paisley, UK). The synthesized cDNAs of the targeted gene (Bcl-xL) and the reference gene (GAPDH) were assessed, using their specific forward and reverse primers and the TakyonTM No Rox SYBR® MasterMix dTTP Blue (Eurogentec, Seraing, Belgium), on a 96-well plate with the CFX96 Real-Time PCR Detection System (BioRad) thermal cycler. GAPDH, an endogenous reference gene, was used as a relative quantification standard to determine the relative expression of Bcl-xL mRNA level in this analysis. The sequence of the specific primers used in this analysis were as follows: forward primer 5′-ATCTCTTTCTCTCCCTTCAG/CTTTCTGGGAAAGCTTGTAG-3′ and reverse primer 5′- TTCAGTGACCTGACATCCCA/TCCACAAAAGTATCCCAGCC-3′ for Bcl-xL and forward primer 5′-CTTTTGCGTCGCCAG/TTGATGGCAACAATATCCAC-3′ and reverse primer 5′- CAAAAGGGTCATCATCTCTGC/AGTTGTCATGGATGACCTTGG-3′ for GAPDH. All specific primers were purchased from Eurogentec (Seraing, Belgium). Non-treated cells and the commercialized transfection reagent (Lipofectamine™ RNAiMAX, Invitrogen, Carlsbad, U.S.A), abbreviated as Lipofectamine, were used as negative and positive controls, respectively. To calculate the relative gene expression of Bcl-xL in each sample, the ΔΔCq method was applied. In this method, the number of quantification cycles (Cq) of the targeted gene (Bcl-xL) and that of the reference gene (GAPDH) of each sample were obtained after qPCR. For each replica, the expression of the Bcl-xL gene was normalized to GAPDH gene expression levels to determine ΔCq ($\Delta Cq = Cq_{(Bcl\text{-}xL)} - Cq_{(GAPDH)}$). The ΔCq was averaged and then normalized to that of the non-treated cells to determine the ΔΔCq ($\Delta\Delta Cq = \Delta Cq_{(sample)} - \Delta Cq_{(non\text{-}treated\ cells)}$). The ΔΔCq was then exponentially transformed to find the ΔΔCq expression, which was equal to $2^{-\Delta\Delta Cq}$ (Bustin, 2004). From that, a normalized, relative gene expression value of Bcl-xL was determined.

2.3.5. Western blot analysis

At 48 h after cell transfection, cells were harvested and lysed in a lysis buffer (RIPA buffer + Protease Inhibitor Cocktail, Thermo Fisher Scientific, Rockford, USA). Cell lysates were centrifuged at 20.000 *g* for 20 min at 4 °C, and the protein content in supernatants was determined using a BCA protein assay kit (Sigma-Aldrich Chimie GmbH, St. Quentin Fallavier, France). Equal amounts of protein lysate (around 20 µg of protein) were electrophoretically separated on 4–12% polyacrylamide gels and transferred to nitrocellulose membranes using an iBlot® 2 (life technologies, Carlsbad, CA). After blocking with milk in TBS-Tween 20 1× at 5% (MT) during 1 h, at room temperature and under constant agitation, each membrane was incubated with the anti-BcL-xL monoclonal antibody (Abcam, Cambridge, UK, dilution 1/1000 in MT) or the anti-GAPDH one (ThermoFisher scientific, Rockford, USA, dilution 1/1000 in MT) for 2 h and subsequently incubated for 1 h with the IgG anti-rabbit secondary antibody antibody (ThermoFisher scientific, Rockford, USA, dilution 1/1000 in MT), both at room temperature and under moderate agitation. After washing, bound antibodies were detected by an enhanced chemiluminescence kit using the ECL (Enhanced ChemiLuminescence) solution (ThermoFisher scientific, Rockford, USA). The percentage of the BcL-xL protein expression in each sample was estimated by normalizing to the corresponding GAPDH protein and comparing to those in non-treated cells using the quantification function of Imager Fusion-Solo.65.WL (Vilber Lourmat, Marne-la-Vallée, France).

2.3.6. Apoptosis assay

H460-Luc cells were seeded at 3×10^4 cells/well in 12-well plates for 24 h. NM-scFv anti-Bcl-xL, NM-scFv control at 100 nM in siRNA were then transfected in the similar conditions used in qPCR assays for a final volume of 600 µL/well. For non-treated cells or cells treated with cisplatin alone (a gift from CHU Bretonneau Pharmacy, Tours, France), abbreviated as CIS, the NM-scFv was replaced by the Opti-MEM medium. At 24 h of incubation, 3.66 µL or 11 µL of CIS at 330 µM was added into each well to obtain final concentrations at 2 µM or 6 µM, respectively. After 48 h of incubation, cells were harvested and washed twice with PBS 1× buffer. Annexin V labelled with Alexa™488 and Propidium Iodide (PI) were added according to the recommendation from the manufacturer (Thermo Scientific™). Cells treated with free anti-Bcl-xL siRNAs, NMs-scFv anti-Bcl-xL, or NMs-scFv control in the absence of CIS were used as controls. The proportions of cells in early and late apoptosis were obtained by acquisition of 10,000 cells with MACSQuant®10 flow cytometer (Miltenyi).

2.3.7. Cell viability assay

The IC_{50} values of cisplatin in H460-Luc cells treated or non-treated with NM-scFv were determined to evaluate chemotherapy efficiency. To this end, H460-Luc cells were seeded at 3×10^3 cells/well in 96-well plates for 24 h. After 24 h, the transfection with anti-BcL-xL siRNAs complexed in NM-scFv was performed in the same conditions of qPCR assays but for a final volume of 100 µL/well. For cells treated with CIS alone, the NM-scFv was replaced with the Opti-MEM medium. At 24 h of incubation, 6.5 µL of CIS at 3300 µM, 330 µM, 33 µM, 3.3 µM, 0.33 µM and 1.96 µL of CIS at 330 µM and 33 µM was added into wells to obtain a final range of CIS concentrations of 200, 20, 6.33, 2, 0.633, 0.2, and 0.02 µM. The plate was incubated for another 48 h. After this incubation time, 100 µL of the CellTiter-Glo® reagent (Promega, USA) was added in each well and the luminescence assay was performed using a microplate reader. By comparing the light emission of each sample to that of non-treated cells, the percentage of live cells for each concentration of CIS and in each condition was determined. The IC_{50} values were subsequently calculated and the cell viability was statistically compared using GraphPad Prism® v7 (GraphPad Software, San Diego, U.S.A). For

negative and positive controls, the medium of H460-Luc cells and H_2O_2 at 20 mM were used, respectively. Moreover, another cellular viability test was performed in the same conditions with NM-scFv anti-Bcl-xL, NM-scFv control, non-formulated siRNA anti-Bcl-xL, and NV-scFv and in absence of CIS.

2.4. Statistics

Values were expressed as means ± standard deviations (SD). Differences of cell viability between groups in cell viability assay were compared using the Student's one-tailed *t*-test. The difference was considered significant when the obtained *p*-values were lower than 0.05. All experiments were triplicated and the obtained data were treated with the GraphPad Prism® v7 (GraphPad Software, San Diego, CA, U.S.A).

3. Results and discussion

3.1. Formulation and characterizations of NM-scFv anti-Bcl-xL

3.1.1. Formulation and physico-chemical characterizations

Our NM-scFv formulation was based on the complexation between targeted nanovectors (NVs-scFv), anti-Bcl-xL siRNAs, and two cationic polymers. This nanoformulation can be divided into two principal steps including the synthesis of NVs-scFv and the complexation between these nanovectors, the cationic polymers and anti-Bcl-xL siRNAs (Fig. 1.).

The synthesis of NVs and NVs-scFv was identical to that of our previous publication (Vinh Nguyen et al., 2020). As expected, the physico-chemical properties of the obtained NV and NV-scFv (size around 75 nm and slightly negatively charged around −2 mV) were comparable to those previously described (Table SI 1). These results prove that the synthesis pathway is highly reproducible, which sets a strong basis for further scale-up.

Afterwards, the NVs and NVs-scFv were complexed with anti-Bcl-xL siRNAs, chitosan and PLR using the optimized component ratios, which had been obtained previously (Vinh Nguyen et al., 2020). Table 1 showed the colloidal properties of the NMs and the NMs-scFv anti-Bcl-xL. All NMs and NMs-scFv were approximately 100 nm in size, with a low polydispersity index (<0.3), and bare slightly positive charges. These physico-chemical properties are suitable for intravenous injection (IV) and similar to those of NMs or NMs-scFv formulated with control siRNA, reflecting a high reproducibility for our formulation with different kinds of siRNAs (Vinh Nguyen et al., 2020). According to the literature, current siRNA delivery systems using electrostatic forces are usually challenged by the lack of reproducibility and a large size of the finalized complex (Ben Djemaa et al., 2019). At this point, our NM-scFv system presents several advantages including i) a good reproducibility for several sequences of siRNAs and ii) a smaller size and a higher monodispersity for IV administration. Taking a previous study of our team with NMs functionalized with cell penetrating peptide (CPP) but using similar components (SPIONs, chitosan, PLR and siRNA) as an example, the obtained NMs had a larger size around 175 nm, a higher PDi of 0.34 and + 14.2 mV in charge (Ben Djemaa et al., 2018). In that study, the component ratios were not similar (MR = 10, CR = 2, CS = 30), leading to another organization of the serval components. In another study of Veiseh et al., the authors used SPIONs covered by polyethylene glycol (PEG)-grafted with chitosan, and polyethylenimine (PEI) to deliver siRNA into cancer cells. Despite the chemical conjugation used in that study, the finalized NMs had a bigger size (111.9 ± 52.4 nm) than that of our NM-scFv. Besides, the authors had to use a double concentration in siRNA (around 200 nM) to obtain a comparable GFP silencing efficiency to that obtained with our NM-scFv (Veiseh et al., 2010; Vinh Nguyen et al., 2020). These results demonstrate the robustness and the high reproducibility level of our formulation in comparison to other nanoplatforms described in the literature for siRNA delivery in spite of their relatively weak electrostatic forces.

Table 1
Physico-chemical properties of NMs and NMs-scFv for anti-Bcl-xL siRNA delivery.

Batch	D_H (nm)	PDi	ζ (mV)
NM anti-Bcl-xL	99.0 ± 2.5	0.27 ± 0.004	+7.7 ± 1.3
NM-scFv anti-Bcl-xL	104.3 ± 2.9	0.25 ± 0.003	+10.0 ± 1.2

3.1.2. siRNA complexation capacity

One of the most challenging issues for the therapeutic applications of siRNAs is their degradation by nucleases (Ben Djemaa et al., 2019). Therefore, an efficient siRNA delivery system must be able to successfully protect siRNAs from nucleases. In a preliminary study, we demonstarted that if siRNAs are fully complexed within our NMs, they will be well protected from the degradation using ribonuclease A (Bruniaux et al., 2017). Therefore, in the current study, we first studied the complexation capacity between our NM-scFv and siRNAs using the electrophoresis assay.

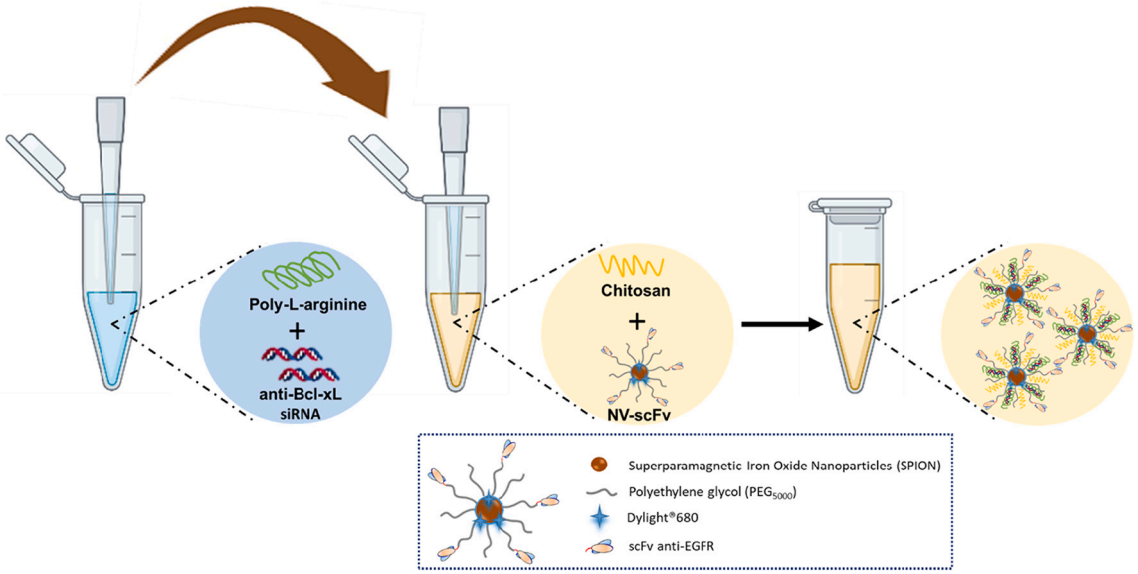

Fig. 1. Schematic representation of NM-scFv anti-Bcl-xL formulation.

In the case of the anti-Bcl-xL siRNA, since we planned to use the siRNA dose at 100 nM and 2000 nM for further *in vitro* and *in vivo* studies respectively, NMs and NMs-scFv anti-Bcl-xL were prepared at 2000 nM for siRNA complexation tests. As shown in Fig. 2A, the gel agarose electrophoresis was made for NMs and NMs-scFv anti-Bcl-xL with/without added heparin. On one hand, without heparin addition, no fluorescent band of free siRNAs was detected for both NMs and NMs-scFv anti-Bcl-xL. On the other hand, when heparin is added, the NMs and NMs-scFv anti-Bcl-xL were destabilized and free siRNAs were liberated. As a result, fluorescent bands corresponding to liberated Bcl-xL siRNAs at the same intensity as naked siRNAs were observed for both NMs and NMs-scFv. All aforementioned results demonstrated that at the siRNA dose of 2000 nM, siRNAs were successfully and completely complexed in our NMs. In the literature, the application of cationic polymers such as chitosan and PLR has been described to be able to complex and protect efficiently siRNAs. For instance, Kim et al. succeeded in formulating nanoparticles *via* electrostatic complexation between negatively-charged hyaluronic acid and cationic poly L-arginine (PLR) and siRNAs. Those obtained NPs were showed to be stable in several serum concentrations and possessed a bigger size than our NM-scFv (Kim et al., 2009).

3.1.3. Targeting and internalization assay into H460-Luc cells

To confirm the active targeting property of anti-EGFR scFv ligands grafted on NM-scFv, cellular uptake levels of NMs and NMs-scFv anti-Bcl-xL into EGFR-overexpressing H460-Luc cells were compared after 24 h of incubation. As shown in Fig. 2B, by monitoring the fluorescence signal of Dylight™680 attached on the inorganic core of the nanovectors, a better internalization level by a factor of 1.5 ($p < 0.01$) was achieved for our targeted NMs-scFv in comparison to that of non-targeted NMs, revealing the *in vitro* active targeting properties of our nanoplatforms. In our previous publication for the same kind of NM-scFv in triple negative breast cancer cells MDA-MB-231, a similar factor of difference was observed (Vinh Nguyen et al., 2020). This observation is really encouraging, as this strategy has been proven potential as a mean to develop a novel nanomedicine able to simultaneously target several kinds of cancers.

3.2. Transfection efficiency of siRNA anti-Bcl-xL in NSCLC cells

3.2.1. Downregulation of Bcl-xL mRNA in cancer cells treated with NM-scFv anti-Bcl-xL

To determine whether anti-Bcl-xL siRNAs were successfully delivered into cancer cells and exerted their activity, a Bcl-xL gene silencing experiment in H460-Luc cells with NMs and NMs-scFv anti-Bcl-xL was performed. The non-targeted and targeted NMs anti-Bcl-xL were incubated with H460 cells for 24 h. After 24 h of transfection, the quantitative PCR (qPCR) technique was used to evaluate the gene silencing effect performed by our NM-scFv and NM anti-Bcl-xL at the mRNA level. To this end, the normalized relative gene expression values of Bcl-xL gene in H460-Luc cells treated with NMs and NMs-scFv anti-Bcl-xL were determined.

As shown in Fig. 3A, our positive control, Lipofectamine, exerted a near perfect gene silencing effect compared to the non-treated cells. Both NMs and NMs-scFv showed a Bcl-xL gene knockdown activity. This result revealed that anti-Bcl-xL siRNAs loaded in either NMs or NMs-scFv were able to cross the membrane barriers, got access to the cytoplasm and performed their interfering activity on the target mRNAs. However, a greater gene silencing activity by a factor of 1.9 was obtained for NMs-scFv compared to NMs ($p < 0.01$), which confirmed the benefit of using anti-EGFR scFv ligands as targeting moieties. In addition, our NMs-scFv have been proven appropriate for IV administration, whereas available commercialized transfection reagents including Lipofectamine are not (Vinh Nguyen et al., 2020). Moreover, the treatment with Lipofectamine was traumatic for the cells, as reflected by abnormal cellular morphology visible under microscope observation after the incubation, whereas such phenomenon was not observed in the case of H460 cells treated with our NM-scFv.

3.2.2. Downregulation of Bcl-xL protein in H460 cells treated with NM-scFv anti-Bcl-xL

At the protein level, Western blot analysis was performed at 48 h after transfection to evaluate the transfection efficiency of our NMs. Fig. 3B illustrates the expression of Bcl-xL protein in H460-Luc cancer cells induced by NMs, NMs-scFv, and Lipofectamine as positive control. A better downregulation activity by a factor of 1.7 was achieved for NMs-scFv compared to NMs. As expected, this transfection efficiency is lower than that of the positive control (62.8% *vs* 84.9%). Nevertheless, our NM-scFv has earned its place among the most effective siRNA

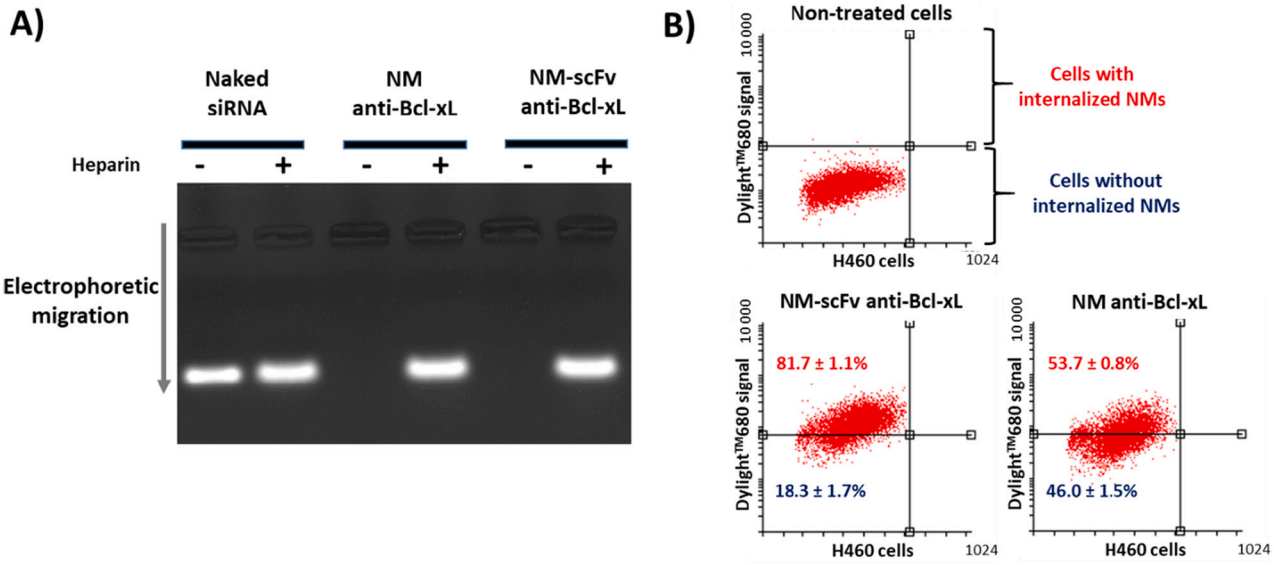

Fig. 2. A) Gel agarose electrophoresis assay to detect free anti-Bcl-xL siRNA in NM and NM-scFv with (+) or without (−) heparin. B) Dylight™680 fluorescence signal of H460-Luc cells non-treated or treated with NM anti-Bcl-xL and NM-scFv anti-Bcl-xL after 24 h of contact. All experiments were in triplicate, and one representative experiment is presented.

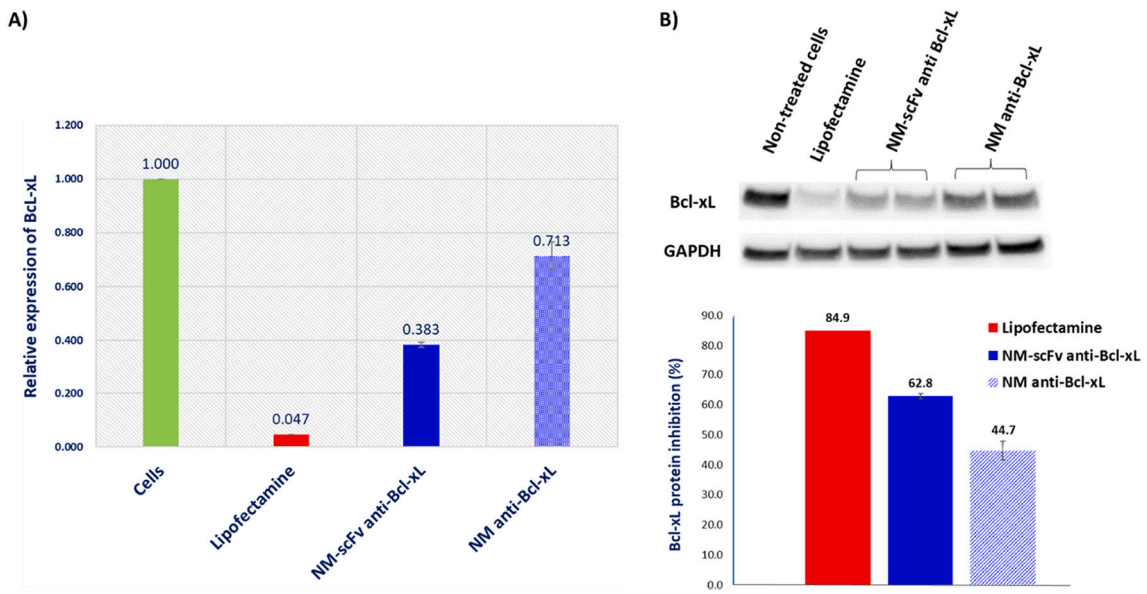

Fig. 3. Bcl-xL mRNA (A) and Bcl-xL protein (B) expression determined by qPCR after 24 h and by Western Blot after 48 h, respectiveley in H460-Luc cells treated with Lipofectamine™RNAimax, NM anti-Bcl-xL or NM-scFv anti-Bcl-xL. Results are the mean values ± SD of three separate experiments.

nanovectors whose transfection efficiency varies from 60% to 88% (Ben Djemaa et al., 2019). In our previous study, a transfection efficiency of around 68% was obtained in triple negative breast cancer cell-line (MDA-MB-231) with a model anti-GFP siRNA (Vinh Nguyen et al., 2020). In these studies, there is a difference in the nature and localization of the target proteins. The GFP gene is artificially introduced into MDA-MB-231 cells and are located in the cell cytoplasm, whereas the Bcl-xL one is mainly present on the outer membrane of mitochondria even if it also present in the cytosol, endoplasmic reticulum and nucleus (Popgeorgiev et al., 2018). As a result, the transfection of anti-Bcl-xL siRNAs are theoretically much more difficult than that of GFP. For example, by using a nanocomplex made of dendrimers functionalized with aptamers as targeting moieties for the delivery of anti-Bcl-xL shRNA, Ayatollahi et al. obtained a reduction of 55% in Bcl-xL expression (Ayatollahi et al., 2017). In another study of Taghavi et al. using targeted carbon nanotubes, a gene silencing effect for Bcl-xL gene of around 41.7% was achieved (Taghavi et al., 2016). In our case, a comparable gene knockdown activity was obtained with our NM-scFv for a new kind of cancer cell-line and a therapeutic siRNA. This result highlights clearly the interest of our nanosystem in the delivery of different kinds of siRNAs. Consequently, this potency may be useful to target simultaneously different cancer-associated genes in regardless of their localization in cancer cells.

3.3. *Synergistic activity of NM-scFv anti-Bcl-xL and cisplatin*

In the literature, the downregulation of the Bcl-xL protein was proven useful when it comes to enhance chemotherapy efficiency in various kinds of cancer including the NSCLC (Andriani et al., 2006; Lei et al., 2007). As the inhibitory activity of our NMs-scFv anti-Bcl-xL was

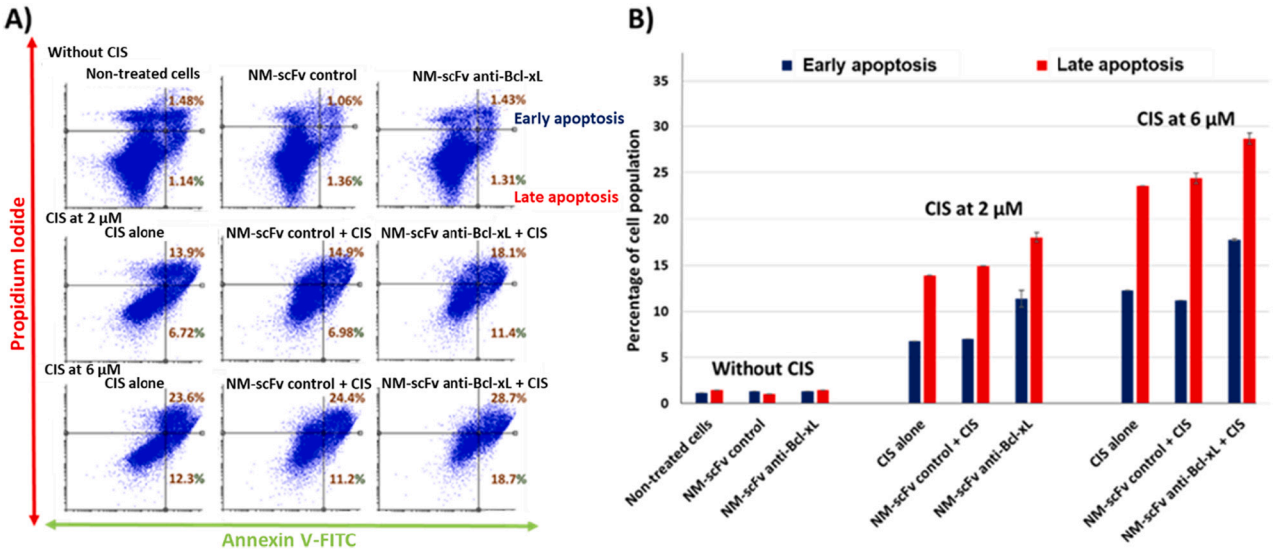

Fig. 4. Apoptosis assay using flow cytometry after staining with annexin V-FITC/propidium iodide (PI). H460 cells were treated with NM-scFv control or NM-scFv anti-Bcl-xL with/without cisplatin. A) Cells were classified as healthy cells (Annexin V−, PI−), early apoptotic cells (Annexin V+, PI−), late apoptotic cells (Annexin V+, PI+), and damaged cells (Annexin V−, PI+). B) Percentage of H460 cells in early and late apoptosis among different treatment options. This experiment was in duplicate and one representative experiment is presented.

proven for H460 cells, their therapeutic activity, especially their synergistic activity with chemotherapeutic agents, were evaluated in the current study. To this aim, the apoptotic and cytotoxic activity of cisplatin (CIS), an anticancer medication normally used as the mainstay for NSCLC treatment, was evaluated in H460-Luc cells, treated either with the combination of our NM-scFv anti-Bcl-xL and CIS or with CIS alone.

3.3.1. Apoptosis assay

Firstly, an apoptosis assay was carried out to determine whether our NM-scFv anti-Bcl-xL can enhance the apoptotic activity of cisplatin (Fig. 4). As shown in the Fig. 4, in absence of cisplatin, all negative controls with NM-scFv anti-Bcl-xl or NM-scFv control did not show any impact on the H460-Luc cells' apoptosis. The cancer cells treated with these formulations presented a negligible proportion of cells entering in the early or in the late apoptosis (around 1%). When cisplatin was added, at both concentrations of 2 μM or 6 μM, a remarkable increase in the cellular population in early apoptosis and in late apoptosis was achieved for the combination of NM-scFv anti-Bcl-xL + cisplatin compared to the use of cisplatin alone (an increase by a factor of 1.7 and 1.3 at 2 μM and a factor of 1.45 and 1.1 at 6 μM, respectively). In addition, at both concentrations of cisplatin, the combination of control NM-scFv formulated with scramble siRNA and cisplatin did not show any impact in the percentage of cells entering in apoptosis, compared to CIS alone. Especially, the apoptotic activity, as mainly reflected by the percentage of cancer cells in early apoptosis, of the combination NM-scFv anti-Bcl-xL + cisplatin at 2 μM was found to be comparable to that of the monotherapy of cisplatin at 6 μM (11.4% *vs* 12.3%, respectively). All these results revealed that: i) without the chemotherapy agent, the NM-scFv anti-Bcl-xL does not have any impact on the apoptosis process of H460-Luc cancer cells in the present treatment scheme, ii) there is a synergistic activity between NM-scFv anti-Bcl-xL + cisplatin that helped to improve the apoptotic or therapeutic activity of this anticancer agent, and iii) the addition of our NM-scFv anti-Bcl-xL in the treatment may help to reduce the CIS dose by a factor of three and is certainly helpful to reduce both its side effects and the emergence of drug resistance.

3.3.2. Cellular viability test

To better confirm the synergistic activity between our NM-scFv anti-Bcl-xL and cisplatin, a cellular viability test was carried out in H460 cells treated with different NMs-scFv (anti-Bcl-xL or control), non-formulated siRNA anti-Bcl-xL or NVs-scFv. As shown in Fig. 5, no cytotoxicity was observed for H460 cells treated with these formulations, reflecting that at the tested concentration of 100 nM in siRNA (13.3 g of iron/L), none of these nanoparticles have an impact on the viability of this cancer cell line. Nevertheless, the IC_{50} value of H460-cells treated with NMs-scFv anti-Bcl-xL siRNA + CIS was effectively and significantly reduced in comparison to those treated with NMs-scFv control + CIS, or CIS alone (0.68 ± 0.12 μM *vs* 3.11 ± 0.17 μM and 2.2 ± 0.18 μM, respectively). In comparison to the study of Lopez-Ayllon et al., the IC_{50} value of CIS for H460 cells was determined to be 1.02 μM, which is lower than that in our study. This difference is probably due to the time dependent activity of CIS. Indeed, Lopez-Ayllon et al. incubated CIS on the cancer cells for 72 h, whereas it was reduced to 48 h in our study (Lopez-Ayllon et al., 2014). Besides, statistical analysis showed that the cellular viability for the cells treated with NMs-scFv anti-Bcl-xL + CIS was significantly lower than that corresponding to single treatment with CIS ($p < 0.01$) and NMs-scFv control + CIS ($p < 0.01$), while no significant difference in the survival rate was obtained between control NMs-scFv + CIS and CIS alone ($p > 0.05$).

These results indicate clearly that the Bcl-xL protein downregulation induced by our NM-scFv anti-Bcl-xL provides a synergistic effect with CIS, in enhancing its cytotoxic activity on H460 cells. The same phenomenon has been also observed in the literature, as the use of gene therapy to down-regulate anti-apoptotic proteins such as Bcl-2 or Bcl-xL were useful to improve the therapeutic activity of different chemotherapeutic drugs in a broad range of tumors (Cao et al., 2007; Kim et al., 2004). For example, in a study of Lei et al., the authors showed that the suppression of Bcl-xL led to a greater growth inhibition of another kind of CIS-resistant lung cancer (A549) cells that demonstrated also the perspective of this strategy (Lei et al., 2007). In another study of Mu et al., the combination of anti-Bcl-xL siRNAs and cisplatin resulted also in a better anticancer activity at *in vivo* level than the monotherapy of cisplatin in prostate cancer (Mu et al., 2009). Besides, the synergistic activity of the combination between other anticancer agents such as doxorubicin and anti-Bcl-xL interfering RNA has been also confirmed (Ebrahimian et al., 2017). One of the most outstanding example was that of Taghavi et al., the authors used targeted carbon nanotubes modified with branched PEI-PEG and aptamers as a vehicle for shRNA delivery in gastric cancer. A reduction of 58.9% in Bcl-xL expression was obtained in cells treated with the targeted nanoparticles. Astonishingly, in combination with doxorubicin, a remarkable synergistic activity was clearly demonstrated, as reflected by a remarkable reduction in IC_{50} value by a factor of 58 in cancer cells treated with the targeted NPs in comparison to that of cells treated with free drug (Taghavi et al., 2016). In another study of Kim et al., the authors used PEI-PEG nanoparticles functionalized with aptamers as active targeting for the co-delivery of anti-Bcl-xL shRNAs and doxorubicin. Interestingly, the authors demonstrated that IC_{50} values of such targeted nanoparticles were approximately 17-fold less than those for the mixture of shRNA delivered by lipofectamine and free drug, highlighting the benefit of co-encapsulate anti-cancer drugs and iRNAs within a nanosystem (Kim et al., 2010). Therefore, the encapsulation of an anticancer agent is scheduled for the next step of the current study that may help to better improve the anticancer activity of our targeted NM-scFv.

Furthermore, in some kinds of tumors such as bone cancer, the inhibition of Bcl-xL protein was shown to be more effective to enhance the

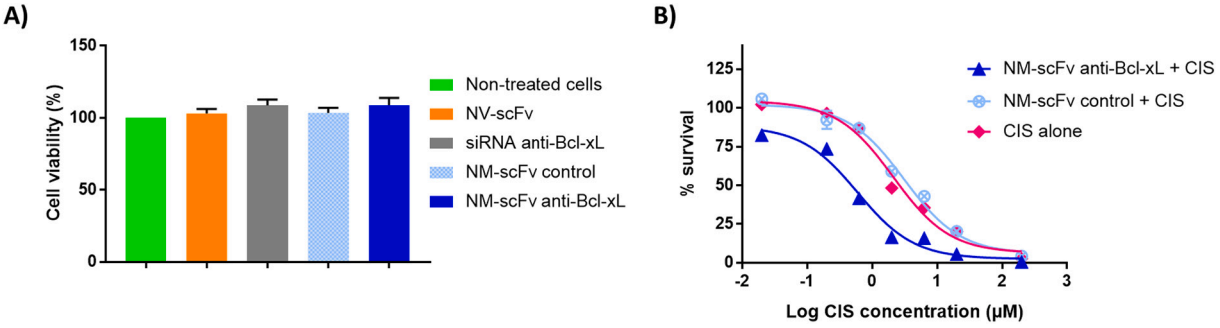

Fig. 5. A) Viability of H460 cells treated with NM-scFv, NV-scFv and non-formulated siRNA at 100 nM in siRNA (13.3 g of iron/L); B) Viability of H460-Luc cells treated with different concentrations of cisplatin (CIS) alone or in combination with NM-scFv anti-Bcl-xL siRNA or NM-scFv control for 48 h of incubation. Results are the mean values ± SD of three separate experiments.

efficiency of chemotherapy than that of Bcl-2 (de Jong et al., 2018). In lung cancer, a study of Leech et al. showed that the treatment of NSCLC cells (A549 cells) with anti-Bcl-xL antisense oligodesoxynucleotides at 600 nM that inhibited from 70% to 90% Bcl-xL expression, had an effective apoptotic activity. In contrast, the same treatment did not show any effect on the apoptosis of small cells lung cancer cells (Leech et al., 2000). These findings reveal that the Bcl-xL inhibition with siRNAs is a specific treatment for the NSCLC. All together, these observations suggest that the role of each member of the Bcl-2 family in each kind of cancer needs to be clarified and the choice of appropriate target proteins is a prerequisite to the treatment success. In our case, thanks to the flexibility in the choice of siRNAs, our nanoformulation is suitable for different kinds of siRNAs and therefore can be used to target different (onco)proteins. In particular, a mix of different siRNAs to target simultaneously different (onco)proteins may be achieved with our nanosystem.

In addition, the synergistic activity between our NM-scFv anti-Bcl-xL and chemotherapy agents may contribute also to the fight against the emergence of resistance by reducing the administration dose of these anticancer agents. Indeed, several studies have revealed that the Bcl-xL overexpression is a frequent phenomenon in cancer and strictly related to the chemoresistance of the NSCLC (Andriani et al., 2006; Lu et al., 2021). Consequently, a new strategy to better exploit the Bcl-xL gene therapy was introduced in this study and might be a potential solution to reduce the CIS dose used in clinical. Especially, in the case of patients with severe side effects caused by CIS, a lower necessary dose can help to improve both drug effectiveness and tolerance. For further studies, the potential of our NM-scFv formulated with Bcl-xL siRNAs in CIS-resistant cancer cells will be evaluated both *in vitro* and *in vivo*.

4. Conclusion

In the frame of this study, a targeted nanomedicine with anti-EGFR scFv moieties was applied for the active delivery of anti-Bcl-xL siRNA into NSCLC cells. The obtained results demonstrate that our NM-scFv anti-Bcl-xL was suitable for IV administration in terms of physico-chemical properties, providing complete complexation with the formulated siRNA, then delivered them actively and efficiently into their active site. Consequently, much greater downregulation of the target gene (Bcl-xL) was achieved in cancer cells treated with our functionalized NM-scFv than in those with the non-functionalized NM, which was confirmed both at the mRNA and protein levels. Ultimately, the synergistic activity of our NM-scFv anti-Bcl-xL in combination with cisplatin was proven *in vitro* in NSCLC H460 cells, as reflected by an enhancement in its apoptotic and cytotoxic activity with a significant reduction by a factor of three in the IC_{50} value of the combination compared to that of the solitary CIS treatment. Furthermore, the high level of reproducibility of this nanoformulation and the capacity of actively targeting a broad range of EGFR-positive cancers are proofs of its potential for *in vivo* and clinical translation in an attempt to reduce the necessary dose of chemotherapy in cancer treatment.

CRediT authorship contribution statement

Phuoc Vinh Nguyen: Conceptualization, Investigation, Writing – original draft. **Katel Hervé-Aubert:** Conceptualization, Funding acquisition, Writing – review & editing, Supervision. **Laurie Lajoie:** Investigation, Writing – review & editing. **Yoann Misericordia:** Investigation, Writing – review & editing. **Igor Chourpa:** Project administration, Writing – review & editing. **Stéphanie David:** Investigation, Writing – review & editing. **Emilie Allard-Vannier:** Conceptualization, Funding acquisition, Writing – review & editing, Supervision.

Declaration of Competing Interest

The authors declare that they have no conflict of interest.

Data availability

The authors do not have permission to share data.

Acknowledgments

The authors would like to thank Dr Nicolas Aubrey and Fanny Boursin (team BioMAP, INRAE 1282, Tours University) for scFv production and characterization. This work was supported by the 'Cancéropôle Grand Ouest' and especially by the Emergence CGO 2019 NANOTIF project. This work was also supported by the French National Research Agency under the program "Investissements d'avenir" Grant Agreement LabEx MAbImprove (ANR-10-LABX-53-01).

Appendix A. Supplementary data

Supplementary data to this article can be found online at https://doi.org/10.1016/j.ijpx.2022.100139.

References

Alexander, M., Kim, S.Y., Cheng, H., 2020. Update 2020: Management of Non-Small Cell Lung Cancer. Lung 198, 897–907. https://doi.org/10.1007/s00408-020-00407-5.
Andriani, F., Perego, P., Carenini, N., Sozzi, G., Roz, L., 2006. Increased Sensitivity to Cisplatin in Non-Small Cell Lung Cancer Cell Lines after FHIT Gene transfer. Neoplasia 8, 9–17. https://doi.org/10.1593/neo.05517.
Ayatollahi, S., Salmasi, Z., Hashemi, M., Askarian, S., Oskuee, R.K., Abnous, K., Ramezani, M., 2017. Aptamer-targeted delivery of Bcl-xL shRNA using alkyl modified PAMAM dendrimers into lung cancer cells. Int. J. Biochem. Cell Biol. 92, 210–217. https://doi.org/10.1016/j.biocel.2017.10.005.
Bade, B.C., Dela Cruz, C.S., 2020. Lung Cancer 2020. Clin. Chest Med. 41, 1–24. https://doi.org/10.1016/j.ccm.2019.10.001.
Ben Djemaa, S., David, S., Hervé-Aubert, K., Falanga, A., Galdiero, S., Allard-Vannier, E., Chourpa, I., Munnier, E., 2018. Formulation and in vitro evaluation of a siRNA delivery nanosystem decorated with gH625 peptide for triple negative breast cancer theranosis. Eur. J. Pharm. Biopharm. Off. J. Arbeitsgemeinschaft Pharm. Verfahrenstechnik EV 131, 99–108. https://doi.org/10.1016/j.ejpb.2018.07.024.
Ben Djemaa, S., Munnier, E., Chourpa, I., Allard-Vannier, E., David, S., 2019. Versatile electrostatically assembled polymeric siRNA nanovectors: can they overcome the limits of siRNA tumor delivery? Int. J. Pharm. 567, 118432 https://doi.org/10.1016/j.ijpharm.2019.06.023.
Bruniaux, J., Djemaa, S.B., Hervé-Aubert, K., Marchais, H., Chourpa, I., David, S., 2017. Stealth magnetic nanocarriers of siRNA as platform for breast cancer theranostics. Int. J. Pharm. 532, 660–668. https://doi.org/10.1016/j.ijpharm.2017.05.022.
Bustin, S.A., 2004. A-Z of Quantitative PCR. International University Line, La Jolla, CA.
Cao, X., Rodarte, C., Zhang, L., Morgan, C.D., Littlejohn, J., Smythe, W.R., 2007. Bcl2/bcl-xl inhibitor engenders apoptosis and increases chemo-sensitivity in mesothelioma. Cancer Biol. Ther. 6, 246–252. https://doi.org/10.4161/cbt.6.2.3626.
de Jong, Y., Monderer, D., Brandinelli, E., Monchanin, M., van den Akker, B.E., van Oosterwijk, J.G., Blay, J.Y., Dutour, A., Bovée, J.V.M.G., 2018. Bcl-xl as the most promising Bcl-2 family member in targeted treatment of chondrosarcoma. Oncogenesis 7, 74. https://doi.org/10.1038/s41389-018-0084-0.
Dhomen, N.S., Mariadason, J., Tebbutt, N., Scott, A.M., 2012. Therapeutic Targeting of the Epidermal Growth factor Receptor in Human Cancer. Crit. Rev. Oncog. 17, 31–50. https://doi.org/10.1615/CritRevOncog.v17.i1.40.
Duma, N., Santana-Davila, R., Molina, J.R., 2019. Non–small cell lung cancer: epidemiology, screening, diagnosis, and treatment. Mayo Clin. Proc. 94, 1623–1640. https://doi.org/10.1016/j.mayocp.2019.01.013.
Ebrahimian, M., Taghavi, S., Mokhtarzadeh, A., Ramezani, M., Hashemi, M., 2017. Co-delivery of Doxorubicin Encapsulated PLGA Nanoparticles and Bcl-xL shRNA using Alkyl-Modified PEI into Breast Cancer Cells. Appl. Biochem. Biotechnol. 183, 126–136. https://doi.org/10.1007/s12010-017-2434-3.
Ferlay, J., Colombet, M., Soerjomataram, I., Parkin, D.M., Piñeros, M., Znaor, A., Bray, F., 2021. Cancer statistics for the year 2020: an overview. Int. J. Cancer 149, 778–789. https://doi.org/10.1002/ijc.33588.
Fire, A., Xu, S., Montgomery, M.K., Kostas, S.A., Driver, S.E., Mello, C.C., 1998. Potent and specific genetic interference by double-stranded RNA in Caenorhabditis elegans. Nature 391, 806–811. https://doi.org/10.1038/35888.
Herbst, R.S., Morgensztern, D., Boshoff, C., 2018. The biology and management of non-small cell lung cancer. Nature 553, 446–454. https://doi.org/10.1038/nature25183.
Huang, Z., Lei, X., Zhong, M., Zhu, B., Tang, S., Liao, D., 2007. Bcl-2 small interfering RNA sensitizes cisplatin-resistant human lung adenocarcinoma A549/DDP cell to cisplatin and diallyl disulfide. Acta Biochim. Biophys. Sin. 39, 835–843. https://doi.org/10.1111/j.1745-7270.2007.00356.x.
Kim, E.S., 2016. Chemotherapy Resistance in Lung Cancer. In: Ahmad, A., Gadgeel, S. (Eds.), Lung Cancer and Personalized Medicine, Advances in Experimental Medicine and Biology. Springer International Publishing, Cham, pp. 189–209. https://doi.org/10.1007/978-3-319-24223-1_10.

Kim, R., Emi, M., Tanabe, K., Toge, T., 2004. Therapeutic potential of antisense Bcl-2 as a chemosensitizer for cancer therapy. Cancer 101, 2491–2502. https://doi.org/10.1002/cncr.20696.

Kim, E.-J., Shim, G., Kim, K., Kwon, I.C., Oh, Y.-K., Shim, C.-K., 2009. Hyaluronic acid complexed to biodegradable poly L-arginine for targeted delivery of siRNAs. J. Gene Med. 11, 791–803. https://doi.org/10.1002/jgm.1352.

Kim, E., Jung, Y., Choi, H., Yang, J., Suh, J.-S., Huh, Y.-M., Kim, K., Haam, S., 2010. Prostate cancer cell death produced by the co-delivery of Bcl-xL shRNA and doxorubicin using an aptamer-conjugated polyplex. Biomaterials 31, 4592–4599. https://doi.org/10.1016/j.biomaterials.2010.02.030.

Leech, S.H., Olie, R.A., Gautschi, O., Simes-Wst, A.P., Tschopp, S., Hner, R., Hall, J., Stahel, R.A., Zangemeister-Wittke, U., 2000. Induction of apoptosis in lung-cancer cells followingbcl-xL anti-sense treatment. Int. J. Cancer 86, 570–576. https://doi.org/10.1002/(SICI)1097-0215(20000515)86:4<570::AID-IJC20>3.0.CO;2-T.

Lei, X., Huang, Z., Zhong, M., Zhu, B., Tang, S., Liao, D., 2007. Bcl-XL small interfering RNA sensitizes cisplatin-resistant human lung adenocarcinoma cells. Acta Biochim. Biophys. Sin. 39, 344–350. https://doi.org/10.1111/j.1745-7270.2007.00286.x.

Liang, Z., Zhang, J., Zeng, X., Gao, J., Wu, S., Liu, T., 2010. Relationship between EGFR expression, copy number and mutation in lung adenocarcinomas. BMC Cancer 10, 376. https://doi.org/10.1186/1471-2407-10-376.

Lochmatter, D., Mullis, P.E., 2011. RNA interference in mammalian cell systems. Horm. Res. Paediatr. 75, 63–69. https://doi.org/10.1159/000322817.

Lopez-Ayllon, B.D., Moncho-Amor, V., Abarrategi, A., Cáceres, I.I., Castro-Carpeño, J., Belda-Iniesta, C., Perona, R., Sastre, L., 2014. Cancer stem cells and cisplatin-resistant cells isolated from non-small-lung cancer cell lines constitute related cell populations. Cancer Med. 3, 1099–1111. https://doi.org/10.1002/cam4.291.

Lu, Y., Bian, D., Zhang, X., Zhang, H., Zhu, Z., 2021. Inhibition of Bcl-2 and Bcl-xL overcomes the resistance to the third-generation EGFR tyrosine kinase inhibitor osimertinib in non-small cell lung cancer. Mol. Med. Rep. 23 (1), 48 https://doi.org/10.3892/mmr.2020.11686.

Mansour, A.M., Abdelrahim, M., Laymon, M., Elsherbeeny, M., Sultan, M., Shokeir, A., Mosbah, A., Abol-Enein, H., Awadalla, A., Cho, E., Sairam, V., Park, T.D., Shahid, M., Kim, J., 2018. Epidermal growth factor expression as a predictor of chemotherapeutic resistance in muscle-invasive bladder cancer. BMC Urol. 18, 100. https://doi.org/10.1186/s12894-018-0413-9.

Min, H.-Y., Lee, H.-Y., 2021. Mechanisms of resistance to chemotherapy in non-small cell lung cancer. Arch. Pharm. Res. 44, 146–164. https://doi.org/10.1007/s12272-021-01312-y.

Mirzaei, S., Gholami, M.H., Hashemi, F., Zabolian, A., Hushmandi, K., Rahmanian, V., Entezari, M., Girish, Y.R., Sharath Kumar, K.S., Aref, A.R., Makvandi, P., Ashrafizadeh, M., Zarrabi, A., Khan, H., 2021a. Employing siRNA tool and its delivery platforms in suppressing cisplatin resistance: Approaching to a new era of cancer chemotherapy. Life Sci. 277, 119430 https://doi.org/10.1016/j.lfs.2021.119430.

Mirzaei, S., Mahabady, M.K., Zabolian, A., Abbaspour, A., Fallahzadeh, P., Noori, M., Hashemi, F., Hushmandi, K., Daneshi, S., Kumar, A.P., Aref, A.R., Samarghandian, S., Makvandi, P., Khan, H., Hamblin, M.R., Ashrafizadeh, M., Zarrabi, A., 2021b. Small interfering RNA (siRNA) to target genes and molecular pathways in glioblastoma therapy: current status with an emphasis on delivery systems. Life Sci. 275, 119368 https://doi.org/10.1016/j.lfs.2021.119368.

Mu, P., Nagahara, S., Makita, N., Tarumi, Y., Kadomatsu, K., Takei, Y., 2009. Systemic delivery of siRNA specific to tumor mediated by atelocollagen: combined therapy using siRNA targeting Bcl-xL and cisplatin against prostate cancer. Int. J. Cancer 125, 2978–2990. https://doi.org/10.1002/ijc.24382.

Osmani, L., Askin, F., Gabrielson, E., Li, Q.K., 2018. Current WHO guidelines and the critical role of immunohistochemical markers in the subclassification of non-small cell lung carcinoma (NSCLC): moving from targeted therapy to immunotherapy. Semin. Cancer Biol. 52, 103–109. https://doi.org/10.1016/j.semcancer.2017.11.019.

Popgeorgiev, N., Jabbour, L., Gillet, G., 2018. Subcellular Localization and Dynamics of the Bcl-2 Family of Proteins. Front. Cell Dev. Biol. 6, 13. https://doi.org/10.3389/fcell.2018.00013.

Salimath, S., Jayaraj, B.S., Mahesh, P.A., 2015. Epidermal growth factor receptor (EGFR) expression in non-small cell lung carcinoma (NSCLC) and survival. In: 11.1 Lung Cancer. Presented at the Annual Congress 2015. European Respiratory Society, p. PA4255. https://doi.org/10.1183/13993003.congress-2015.PA4255.

Singh, A., Trivedi, P., Jain, N.K., 2018. Advances in siRNA delivery in cancer therapy. Artif. Cells Nanomed. Biotechnol. 46, 274–283. https://doi.org/10.1080/21691401.2017.1307210.

Sosa Iglesias, V., Giuranno, L., Dubois, L.J., Theys, J., Vooijs, M., 2018. Drug Resistance in Non-Small Cell Lung Cancer: a potential for NOTCH Targeting? Front. Oncol. 8, 267. https://doi.org/10.3389/fonc.2018.00267.

Subhan, M.A., Torchilin, V.P., 2019. Efficient nanocarriers of siRNA therapeutics for cancer treatment. Transl. Res. 214, 62–91. https://doi.org/10.1016/j.trsl.2019.07.006.

Šutić, M., Vukić, A., Baranašić, J., Försti, A., Džubur, F., Samaržija, M., Jakopović, M., Brčić, L., Knežević, J., 2021. Diagnostic, predictive, and prognostic biomarkers in non-small cell lung cancer (NSCLC) management. J. Pers. Med. 11, 1102. https://doi.org/10.3390/jpm11111102.

Taghavi, S., HashemNia, A., Mosaffa, F., Askarian, S., Abnous, K., Ramezani, M., 2016. Preparation and evaluation of polyethylenimine-functionalized carbon nanotubes tagged with 5TR1 aptamer for targeted delivery of Bcl-xL shRNA into breast cancer cells. Colloids Surf. B: Biointerfaces 140, 28–39. https://doi.org/10.1016/j.colsurfb.2015.12.021.

Tan, X., Lambert, P.F., Rapraeger, A.C., Anderson, R.A., 2016. Stress-Induced EGFR trafficking: Mechanisms, Functions, and Therapeutic Implications. Trends Cell Biol. 26, 352–366. https://doi.org/10.1016/j.tcb.2015.12.006.

Van den Eynde, M., Baurain, J.F., Mazzeo, F., Machiels, J.P., 2011. Epidermal growth factor receptor targeted therapies for solid tumours. Acta Clin. Belg. 66, 10–17. https://doi.org/10.2143/ACB.66.1.2062508.

Veiseh, O., Kievit, F.M., Fang, C., Mu, N., Jana, S., Leung, M.C., Mok, H., Ellenbogen, R. G., Park, J.O., Zhang, M., 2010. Chlorotoxin bound magnetic nanovector tailored for cancer cell targeting, imaging, and siRNA delivery. Biomaterials 31, 8032–8042. https://doi.org/10.1016/j.biomaterials.2010.07.016.

Vinh Nguyen, P., Hervé-Aubert, K., David, S., Lautram, N., Passirani, C., Chourpa, I., Aubrey, N., Allard-Vannier, E., 2020. Targeted nanomedicine with anti-EGFR scFv for siRNA delivery into triple negative breast cancer cells. Eur. J. Pharm. Biopharm. S0939641120303040 https://doi.org/10.1016/j.ejpb.2020.10.004.

Vinh Nguyen, P., Allard-Vannier, E., Chourpa, I., Hervé-Aubert, K., 2021. Nanomedicines functionalized with anti-EGFR ligands for active targeting in cancer therapy: biological strategy, design and quality control. Int. J. Pharm. 120795 https://doi.org/10.1016/j.ijpharm.2021.120795.

Zhang, Z., Jin, F., Lian, X., Li, M., Wang, G., Lan, B., He, H., Liu, G.-D., Wu, Y., Sun, G., Xu, C.-X., Yang, Z.-Z., 2018. Genistein promotes ionizing radiation-induced cell death by reducing cytoplasmic Bcl-xL levels in non-small cell lung cancer. Sci. Rep. 8, 328. https://doi.org/10.1038/s41598-017-18755-3.